RADIO SCIENCE

Volume 38 Number 1 January - February 2003

Published by
American Geophysical Union
Cosponsored by
International Union of Radio Sciences

U.R.S.I.

RADIO SCIENCE Volume 38, Number 1 January–February 2003

Contents

(continued on inside back cover)

(continued from outside back cover)

Author and DOI Indices appear at the end of the issue

To learn more about How to Cite an article correctly, go to www.agu.org/pubs/reports/eos13aug.htm

To learn more about AGU's publishing strategies, go to www.agu.org/pubs/elecPub.html

To find the print issue in which an article is published this year, use the **DOI Resolver** from the journal home page or go to www.agu.org/pubs/doifind.html

RADIO SCIENCE, VOL. 38, NO. 1, 1001, doi:10.1029/2000RS002604, 2003

Modeling the effects of ionospheric scintillation on GPS/Satellite-Based Augmentation System availability

Robert S. Conker, M. Bakry El-Arini, Christopher J. Hegarty, and Thomas Hsiao

Center for Advanced Aviation System Development, The MITRE Corporation, McLean, Virginia, USA

Received 10 January 2001; revised 3 December 2001; accepted 1 April 2002; published 2 January 2003.

[1] Ionospheric scintillation is a rapid change in the phase and/or amplitude of a radio signal as it passes through small-scale plasma density irregularities in the ionosphere. These scintillations not only can reduce the accuracy of GPS/Satellite-Based Augmentation System (SBAS) receiver pseudorange and carrier phase measurements but also can result in a complete loss of lock on a satellite. In a worst case scenario, loss of lock on enough satellites could result in lost positioning service. Scintillation has not had a major effect on midlatitude regions (e.g., the continental United States) since most severe scintillation occurs in a band approximately 20° on either side of the magnetic equator and to a lesser extent in the polar and auroral regions. Most scintillation occurs for a few hours after sunset during the peak years of the solar cycle. Typical delay locked loop/phase locked loop designs of GPS/SBAS receivers enable them to handle moderate amounts of scintillation. Consequently, any attempt to determine the effects of scintillation on GPS/SBAS must consider both predictions of scintillation activity in the ionosphere and the residual effect of this activity after processing by a receiver. This paper estimates the effects of scintillation on the availability of GPS and SBAS for L1 C/A and L2 semicodeless receivers. These effects are described in terms of loss of lock and degradation of accuracy and are related to different times, ionospheric conditions, and positions on the Earth. Sample results are presented using WAAS in the western hemisphere. *INDEX TERMS:* 6974 Radio Science: Signal processing; 6994 Radio Science: Instruments and techniques; 2439 Ionosphere: Ionospheric irregularities; *KEYWORDS:* ionosphere, scintillation, GPS, SBAS

Citation: Conker, R. S., M. B. El-Arini, C. J. Hegarty, and T. Hsiao, Modeling the effects of ionospheric scintillation on GPS/Satellite-Based Augmentation System availability, *Radio Sci.*, *38*(1), 1001, doi:10.1029/2000RS002604, 2003.

1. Introduction

[2] Ionospheric scintillation is a rapid change in the phase and/or amplitude of a radio signal as it passes through small-scale plasma density irregularities in the ionosphere. These scintillations both reduce the accuracy of GPS/Satellite-Based Augmentation System (SBAS) receiver pseudorange and carrier phase measurements, and can result in a complete loss of lock on a satellite. SBAS is an augmentation system to GPS and will be used for navigation and precision approach. It consists mainly of three systems: (1) the U.S. Wide-Area Augmentation System (WAAS), (2) the European Geostationary Navigation Overlay System (EGNOS), and (3) the Japanese MTSAT (Multifunctional Transport SATellite) Satellite-Based Augmentation System (MSAS). Information on these systems and technical descriptions of the GPS signals are given by *Walter and El-Arini* [1999] and *Parkinson and Spilker* [1996].

[3] Typical delay locked loop (DLL)/phase locked loop (PLL) designs of GPS/SBAS receivers enable them to handle moderate amounts of scintillation. Scintillation has not been seen to have a major effect on midlatitude regions, however, for operations in a band 20 deg on either side of the magnetic equator, scintillation effects on GPS/SBAS receiver performance must be determined.

[4] Previous work in this area [*Hegarty et al.*, 1999; *Pullen et al.*, 1998] defined a statistical model of scintillation signal coupled with a model of receiver processing for L1 (1575.42 MHz) GPS and SBAS carrier and code tracking loops as well as semicodeless L2 (1227.6 MHz) carrier and Y-code tracking capabilities [*Woo*, 2000]. Also, an impressive research effort was described by *Knight and Finn* [1998] in their work to

0048-6604/03/2000RS002604$11.00

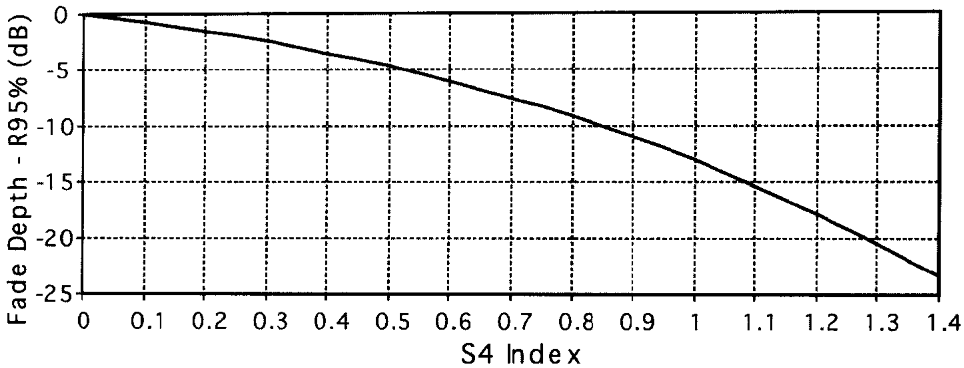

Figure 1. Relationship between S_4 and $R_{95\%}$.

model carrier phase tracking errors and code phase errors in terms of scintillation parameters produced by the well-known wide-band scintillation model WBMOD [*Secan et al.*, 1997] (WBMOD was developed by researchers at Northwest Research Associates, Inc. (NWRA), and funded by several government agencies). This research created an ability to determine the effects of scintillation on GPS receivers. A hardware bench testing for scintillation is being conducted by *Morrissey et al.* [2000] for GPS/SBAS receivers.

[5] The purpose of this paper is to describe the status of research on modeling scintillation effects on GPS/SBAS reference and user receivers' performance. This is summarized as follows: (1) Develop a receiver model that includes the effects of scintillation on tracking performance, (2) estimate the effects of scintillation on navigation service availability, (3) estimate the degree that ionospheric scintillation presents a problem for the operation of the GPS in general and SBAS in particular, and (4) develop an ionospheric scintillation prediction capability for GPS/SBAS availability models [*Poor et al.*, 1999].

2. Background and Approach

2.1. Scintillation Propagation Model

[6] The propagation model implemented in WBMOD is described by *Secan et al.* [1997]. Scintillation estimates are given in terms of a power spectral density (PSD) of phase scintillation of the form $S_{\phi_p}(f) = Tf^{-p}$ where f is frequency (Hz) (greater than or equal to a cutoff frequency), T is a strength parameter (rad^2/Hz) corresponding to the PSD value at 1 Hz, and p is a unitless slope. Also produced are intensity-scintillation parameters $R_{95\%}$ and S_4, which are, respectively the 95th percentile fade depth (dB) and the dimensionless standard deviation of the signal power normalized to the average received power. $R_{95\%}$ and S_4 and are related as shown in Figure 1. This relationship is established through the Nakagami-m distribution [*Nakagami*, 1960].

[7] Scintillation in the ionosphere varies according to Sunspot Number (SSN), geomagnetic index ($0 \leq Kp \leq 9$), time of year, time of day, and geographical position. A receiver's ability to cope with scintillation will be affected by these factors, and the azimuth and elevation of the observed satellite which indicate what part and how much of the ionosphere a radio signal must pass through. It is not possible to show the effects of all of these parameters in one plot, but in order to get a general understanding of the extent of scintillation, a plot has been constructed depicting S_4, a widely used representation of amplitude fading. Figure 2 (produced by WBMOD) depicts S_4 globally with no geomagnetic storms (i.e., Kp = 1) for an ionosphere with SSN = 150, about the peak of the solar cycle. Thus, this figure shows a nominal level ionospheric scintillation undisturbed by storms. The day of the year is September 15 with local time 9:00 P.M. everywhere on the planet. This unusual representation is chosen since scintillation tends to peak after sunset. Consequently, Figure 2 tends to show the maximum effects of S_4 for this day and these ionospheric conditions. Clearly shown is the multimodal distribution of severe scintillation around the magnetic equator, light scintillation in the midlatitude regions and moderate scintillation in the polar and auroral regions. A value of 0 for S_4 indicates no scintillation while a value of 1 indicates severe scintillation.

2.2. Approach

[8] The approach of this study is to generate estimates of ionospheric scintillation related to different ionospheric conditions, times and locations and determine what effect would be seen by a user receiver after receiver processing. The approach is summarized as follows: (1) Use the WBMOD to obtain the scintillation parameters as a function of ionospheric conditions, day of year, and time of day, (2) develop a GPS/SBAS receiver model sensitive to amplitude and phase scintil-

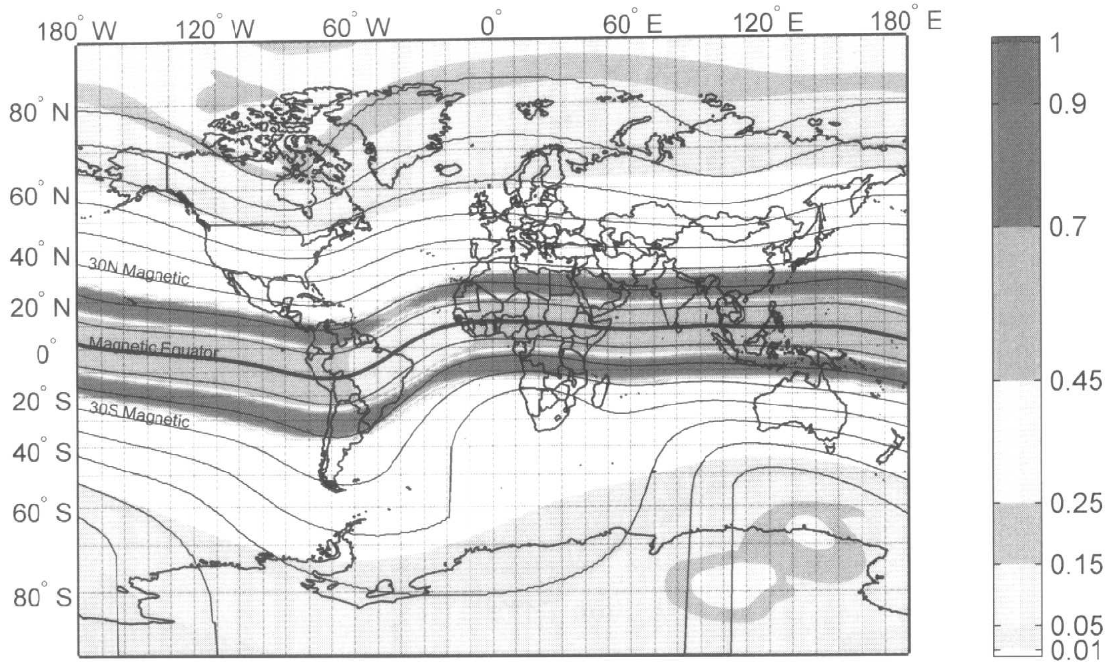

Figure 2. S_4 scintillation parameter for September 15 (95th percentile) (SSN = 150; Kp = 1; local time = 9pm everywhere).

lation, (3) calculate the output of the DLL and PLL of the receiver as a function of the receiver parameters as well as the scintillation signal parameters, and (4) use these results in a GPS/SBAS availability model [*Poor et al.*, 1999] to examine the impact on service availability for different phases of flight.

2.3. GPS/SBAS Receiver Description

[9] A block diagram of a typical GPS C/A-code receiver is shown in Figure 3 [*Ward*, 1994; *Hegarty et al.*, 2001]. The RF signal is received by an L-band antenna. This signal is filtered and then amplified by a low-noise amplifier (LNA). Next, the signal is down-converted to a convenient intermediate frequency (IF) and converted from analog to digital (A/D). The digital signal is then passed to a bank of N channels (see Figure 4 [*Ward*, 1994]) that form complex sums of the correlation between the input signal and C/A code replicas. One channel is needed for each satellite to be tracked. The complex correlation sums are used by a processing unit to track the code and carrier of the received signals so that

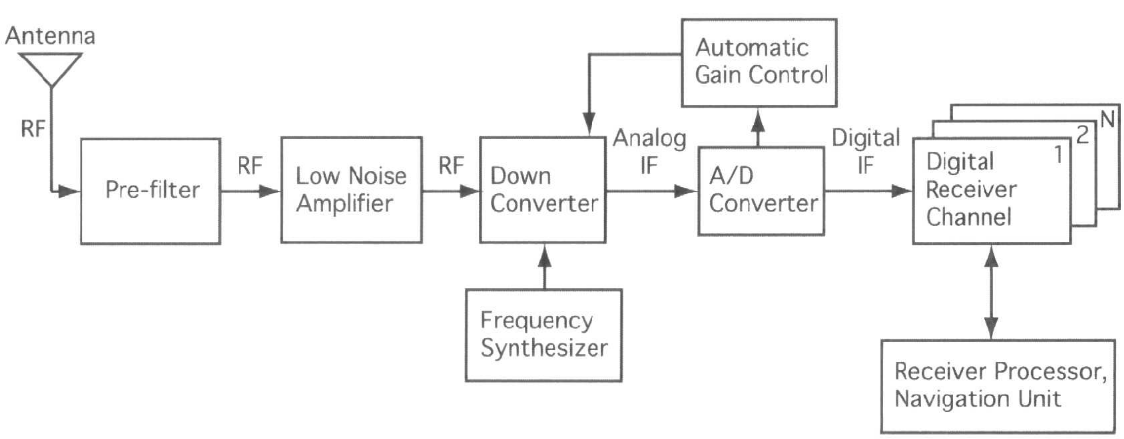

Figure 3. GPS receiver overview.

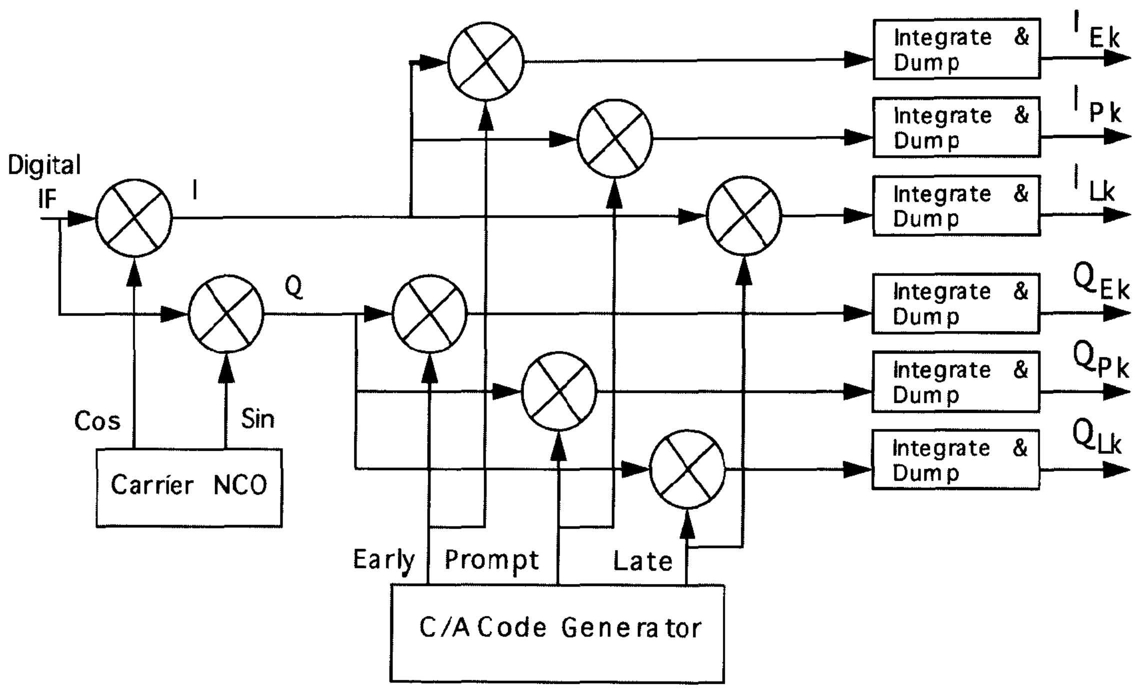

Figure 4. Receiver channel.

pseudoranges to each satellite can be estimated. The correlation sums are also used by the processor to demodulate the data.

[10] In this paper, we model L1 GPS/SBAS C/A code processing and semicodeless GPS L1 and L2 Y-code processing using a baseband model [*Van Dierendonck et al.*, 1992; *Van Dierendonck*, 1996] that starts with the complex correlation sums produced by the generic receiver channel shown in Figure 3. For C/A code processing, the integration periods of 20 ms for GPS and 2 ms for SBAS are used. For semicodeless Y-code processing, the received signals on L1 and L2 are correlated with the P-code over an integration period of 1.96 μs (the deduced period of the underlying encryption code [*Hatch et al.*, 1992]).

[11] The WBMOD generated parameters T, p, and S_4 will be used in a GPS/SBAS receiver model to calculate the code and carrier tracking errors. Specifically, the following will be determined: (1) standard deviation of carrier phase tracking errors for a third-order PLL for L1 GPS and SBAS (to indicate loss of lock), (2) standard deviation of carrier phase errors for a second-order PLL for L2 GPS semicodeless carrier tracking aided by L1 (to indicate loss of lock), (3) standard deviation of code tracking errors from a first-order DLL for L1 GPS and SBAS C/A code (to indicate degradation of accuracy), and (4) standard deviation of code tracking errors from a first-order DLL for L2 GPS semicodeless carrier aided by L1 (to indicate degradation of accuracy).

3. Receiver Modeling

3.1. Computing Signal-to-Noise Ratio

[12] GPS/SBAS receivers can tolerate moderate amounts of ionospheric scintillation. Consequently, a model of receiver processing must be constructed in order to calculate the residual effects on signal amplitude and phase after receiver processing and in the presence of scintillation. An L1 C/A code signal can be received by the user from either an SBAS Geostationary Earth Orbiting (GEO) satellite or a GPS satellite. The received power from these sources at a point on or near the earth's surface is specified in references [*U.S. Air Force*, 1993; *RTCA, Inc.*, 2001, p. A-3] and is shown in Figure 5. The first step in determining signal-to-noise ratio is to linearly estimate the user received signal, C in dBW, from these curves.

[13] The minimum signal levels are those required at the end of a satellite's projected lifetime. The Block II/IIA satellites have exceeded the specified levels, in average, by 3.3 dB for L1-C/A, 6.3 dB for L1P, and 5.4 dB for L2P [*Fisher and Ghassemi*, 1999]. (For future Block IIF satellites, the signal level of L2P is projected to

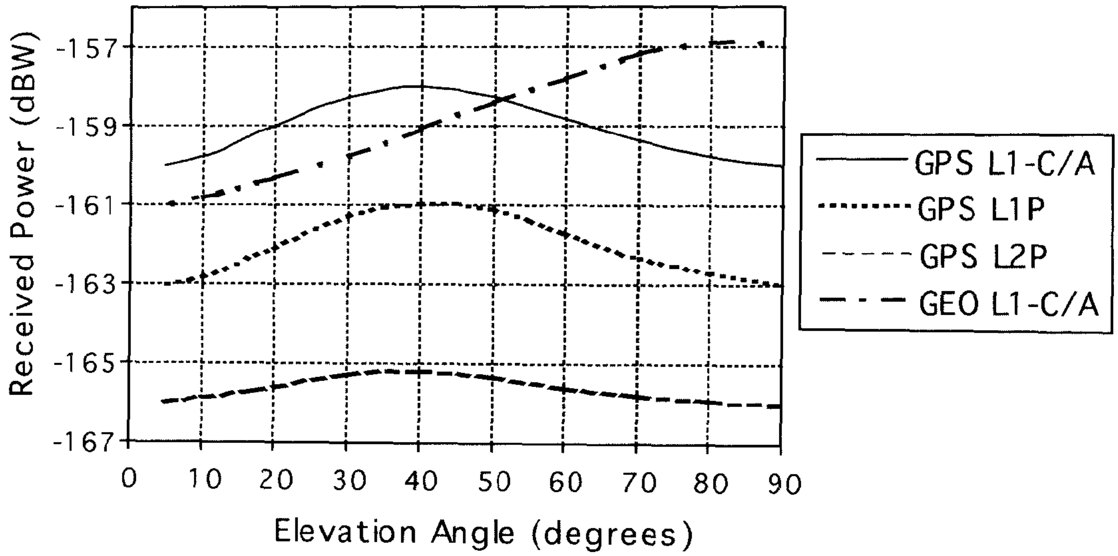

Figure 5. User received minimum signal levels.

be even higher.) We have chosen to add a conservative 3 dB to the minimum signal levels across the entire elevation angle spectrum (5 to 90 deg). Antenna gain, G_a (dBic), is linearly estimated from values in the curve shown in Figure 6. This curve was constructed from the minimum antenna gain values specified in the RTCA GPS Antenna Minimum Operational Performance Standards (MOPS) [*RTCA, Inc.*, 1995]. Actual L1 and L2 antenna gain patterns for a typical, commercial antenna are shown in reference [*Van Dierendonck*, 1996].

[14] The signal-to-noise density ratios for L1-C/A, L1 P-code, and L2 P-code expressed in dB-Hz are respectively [*Conker et al.*, 2000]:

$$(C/N_0)_{L1-C/A} = C_{L1-C/A} + B + G_a + L - (N_0 + I)$$
$$= 10\log_{10}(c/n_0)_{L1-C/A}$$
$$(C/N_0)_{L1P} = C_{L1P} + B + G_a + L - (N_0 + I)$$
$$= 10\log_{10}(c/n_0)_{L1P}$$
$$(C/N_0)_{L2P} = C_{L2P} + B + G_a + L - (N_0 + I)$$
$$= 10\log_{10}(c/n_0)_{L2P}$$

where $C_{L1\text{-}C/A}$, C_{L1P}, C_{L2P} is the minimum required signal power (dBW) at receiver for L1-C/A, L1P, and

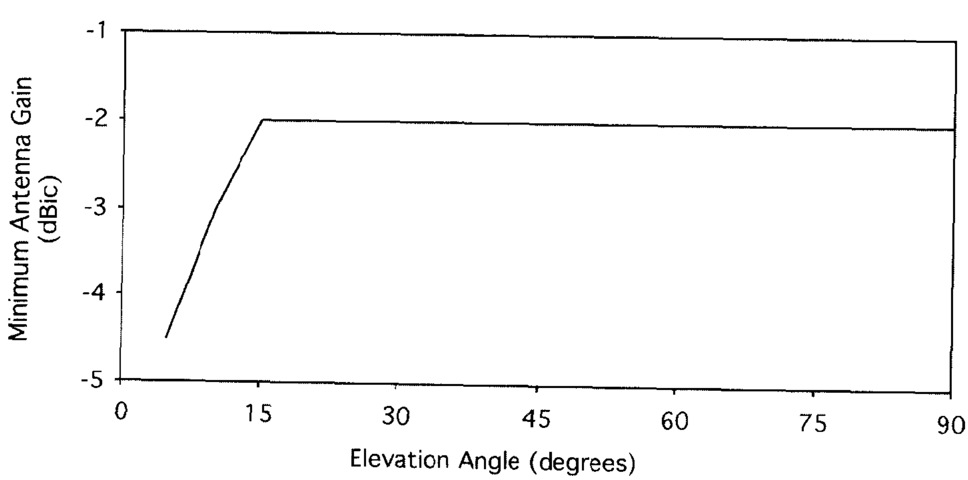

Figure 6. Minimum antenna gain.

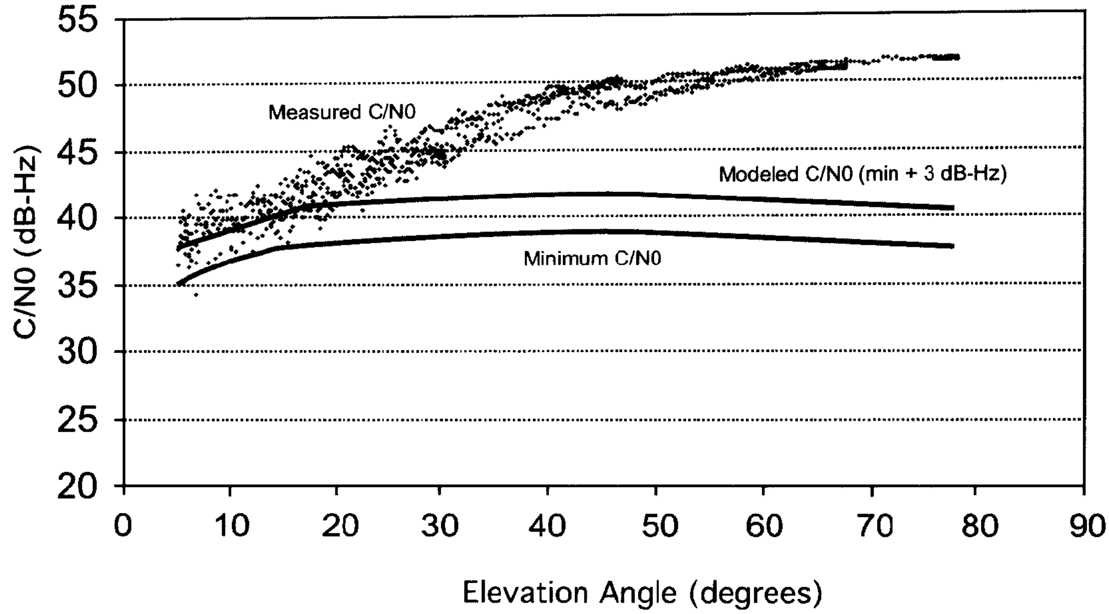

Figure 7. $(C/N_0)_{L1\text{-}C/A}$ for Millennium WAAS receiver.

L2P; B is the difference between typical observed signal strength and minimum specified strength (3 dB); G_a is the antenna gain (dBic); L is the receiver loss (dB), equal to -2.5 dB; N_0 is the noise density, equal to -201.5 dBW-Hz; I is the interference level, equal to 0 dB; and $(c/n_0)_{L1\text{-}C/A}$, $(c/n_0)_{L1P}$, $(c/n_0)_{L2P}$ is the fractional forms of signal-to-noise ratio for L1-C/A, L1P, and L2P.

[15] As a point of interest, receivers may in general achieve even higher signal levels than 3 dB above minimum due to the difference between typical antenna gains and the minimum specified by *RTCA, Inc.* [1995]. Two hours of data for $(C/N_0)_{L1\text{-}C/A}$ and $(C/N_0)_{L2P}$ were recently extracted from the Millennium WAAS receiver. Figures 7 and 8 show respectively the values for (C/N_0) achieved for different elevation angles. Plotted against these measured values are the C/N_0 levels corresponding to the minimum received power levels and the modeled C/N_0 levels with 3 dB added.

[16] The scintillation parameter for L1, $S_4(L1)$, is part of the output of WBMOD. The equivalent parameter for

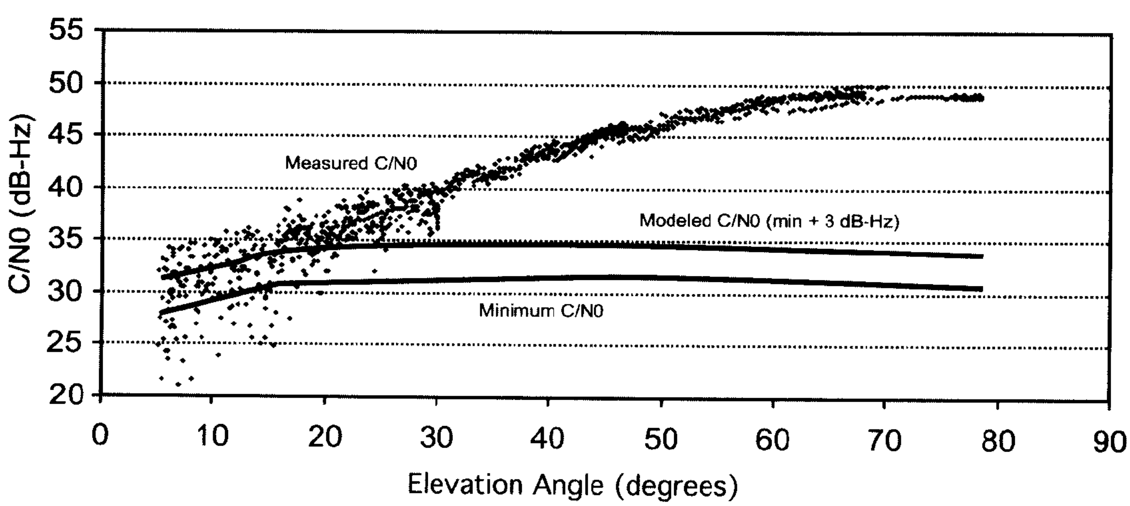

Figure 8. $(C/N_0)_{L2P}$ for Millennium WAAS receiver.

L2 could be determined by executing WBMOD for L2. Instead it is easier to determine $S_4(L2)$ from $S_4(L1)$ by the relationship [*Hegarty et al.*, 1999] based on the frequencies of L1 and L2:

$$S_4(L2) = S_4(L1)\left(\frac{f_1}{f_2}\right)^{1.5} = 1.454 S_4(L1)$$

The receiver can lose lock because of a large phase tracking error. The next two sections will present models for calculating these phase errors for two types of PLLs: a third-order L1 GPS and SBAS carrier PLL, and a second-order L2 semicodeless carrier aided by L1 PLL.

3.2. Determining Tracking Error Variance at Output of PLL for L1 GPS and SBAS Carrier

[17] Assuming no correlation between amplitude and phase scintillation, tracking error variance at the output of the PLL can be computed as follows [*Knight and Finn*, 1998; *Hegarty*, 1997]:

$$\sigma^2_{\Phi_\varepsilon} = \sigma^2_{\Phi S} + \sigma^2_{\Phi T} + \sigma^2_{\Phi,osc} \tag{1}$$

where $\sigma^2_{\Phi S}$, $\sigma^2_{\Phi T}$ and $\sigma^2_{\Phi,osc}$ are respectively the phase scintillation, thermal noise, and the receiver/satellite oscillator noise components of the tracking error variance ($\sigma_{\Phi,osc}$ is assumed to be equal to 0.1 rad (5.7 deg)) [*Hegarty*, 1997]. For simplicity, we neglect phase variance due to other error sources, e.g., multipath. Thermal noise and oscillator noise constitute a lower bound on carrier phase tracking error since, if there is no scintillation, $\sigma^2_{\Phi S} = 0$. Thermal noise tracking error in the presence of scintillation is derived by *Conker et al.* [2000] and is given as follows:

$$\sigma^2_{\Phi_T} = \frac{B_n\left[1 + \frac{1}{2\eta(c/n_0)_{L1-C/A}\left(1-2S_4^2(L1)\right)}\right]}{(c/n_0)_{L1-C/A}\left(1 - S_4^2(L1)\right)} \tag{2}$$

where

- B_n L1 third-order PLL one-sided bandwidth, equal to 10 Hz;
- $(c/n_0)_{L1\text{-}C/A}$ fractional form of C/A code signal-to-noise density ratio, equal to $10^{0.1(C/N_0)_{L1-C/A}}$
- η predetection integration time, equal to 0.02 s for GPS and 0.002 s for WAAS;
- $S_4(L1) < 0.707$.

When there is no scintillation $S_4(L1) = 0$, and the above equation becomes the standard thermal noise tracking error for the PLL [*Hegarty et al.*, 1999]:

$$\sigma^2_{\Phi_T} = \frac{B_n}{(c/n_0)_{L1-C/A}}\left[1 + \frac{1}{2\eta(c/n_0)_{L1-C/A}}\right].$$

From *Rino* [1979] we see that the PSD of phase scintillation can be represented as:

$$S_{\Phi_p}(f) = \frac{T}{(f_0^2 + f^2)^{p/2}} \text{ radians}^2/\text{Hz}$$

where f_0 is the frequency corresponding to the maximum irregularity size in the ionosphere, T is the spectral strength at 1 Hz, and p is the slope of the PSD for $f \gg f_0$. The phase error at the input of the PLL is given by *Rino* [1979]:

$$\sigma^2_{\Phi} = 2\int_{\tau_c}^{\infty} S_{\Phi_p}(f)df$$

where τ_c is a system parameter relating to the phase stability time of the receiver. The phase variance of the carrier phase tracking error is given by *Knight and Finn* [1998]:

$$\sigma^2_{\Phi_S} = \int_{-\infty}^{\infty} |1 - H(f)|^2 S_{\Phi_p}(f)df = T\int_{-\infty}^{\infty} \frac{|1 - H(f)|^2}{(f_0^2 + f^2)^{p/2}}df$$

where

$$|1 - H(f)|^2 = \frac{f^{2k}}{f^{2k} + f_n^{2k}}$$

represents common closed loop transfer functions of the PLL with k, the loop order, equal to 1, 2, or 3 and f_n the loop natural frequency (Hz). Therefore,

$$\sigma^2_{\Phi_S} = T\int_{-\infty}^{\infty}\left(\frac{f^{2k}}{f^{2k} + f_n^{2k}}\right)\left(\frac{1}{(f_0^2 + f^2)^{p/2}}\right)df \tag{3}$$

Both *Rino* [1979] and *Knight and Finn* [1998] considered the case where $f \gg f_0$, in which case an approximation can be made by substituting 0 for f_0, obtaining

$$S_{\Phi_p}(f) = T\left(\frac{1}{(f_0^2 + f^2)^{p/2}}\right) \cong Tf^{-p}$$

The phase variance at the input of the receiver PLL is then approximately

$$\sigma^2_{\Phi} \cong 2T\int_{\tau_c^{-1}}^{\infty} f^{-p}df$$

Further substituting into equation (3):

$$\sigma^2_{\Phi_S} \cong 2T\int_0^{\infty}\frac{f^{2k-p}}{(f^{2k} + f_n^{2k})}df$$
$$= \frac{\pi T}{kf_n^{p-1}\sin\left(\frac{[2k-1-p]\pi}{2k}\right)}, \text{ for } 1 < p < 2k \tag{4}$$

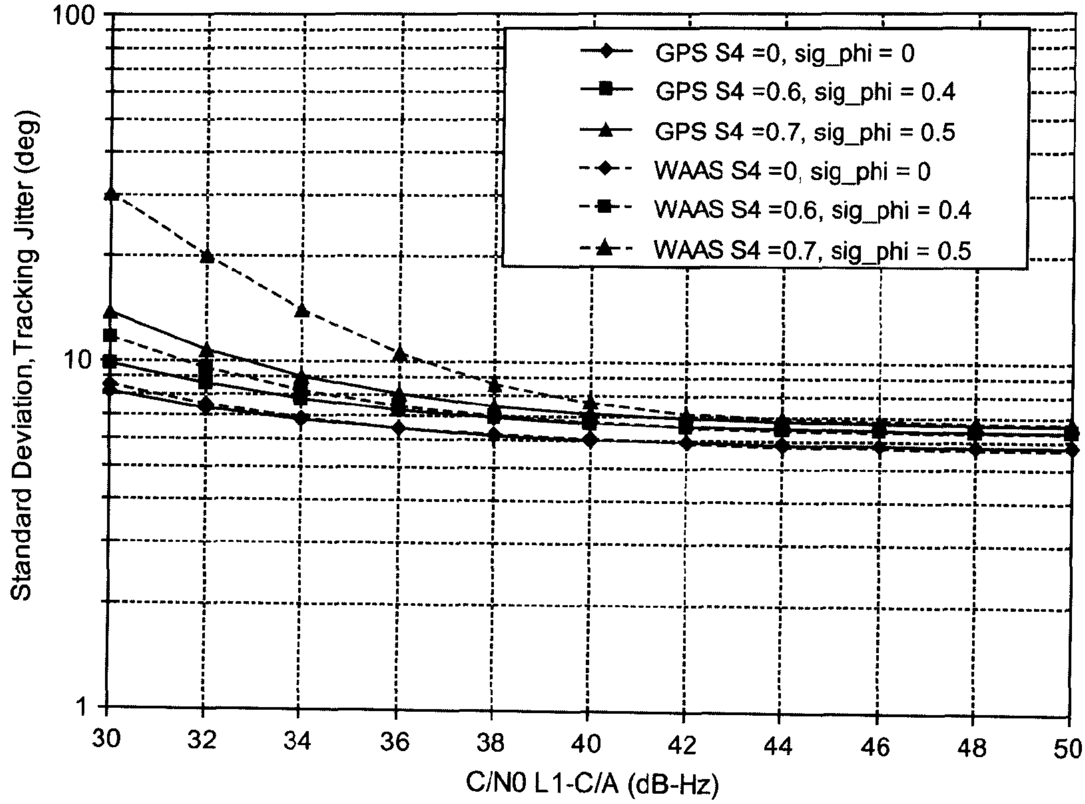

Figure 9. Standard deviation of the tracking jitter for L1 carrier (GPS and WAAS).

which is legitimate as long as $2k - p > 0$ and $p > 1$. Considering that p is generally in the range between 1 and 4, the requirement is met for both third- and second-order loops. For a third-order loop, $k = 3$ and $f_n = 1.91$ Hz [*Van Dierendonck*, 1996]. *Knight and Finn* [1998] maintain that this approximation is fairly accurate.

[18] Finally, from (1), (2), and (4), the phase tracking error variance (rad^2) including scintillation and thermal noise becomes ($1 < p < 2k$):

$$\sigma^2_{\phi_\varepsilon} = \frac{\pi T}{k f_n^{p-1} \sin\left(\frac{[2k+1-p]\pi}{2k}\right)} + \frac{B_n\left[1 + \frac{1}{2\eta(c/n_0)_{L1\text{-}C/A}\left(1-2S_4^2(L1)\right)}\right]}{(c/n_0)_{L1-C/A}\left(1 - S_4^2(L1)\right)} + \sigma^2_{\phi.osc} \qquad (5)$$

Figure 9 shows the standard deviation of the tracking jitter for L1 carrier using equation (5) for both GPS and WAAS.

3.3. Receiver PLL Threshold

[19] An important carrier loop performance measure for many GPS applications is the mean time between cycle slips (called the mean time to lose lock). The mean time between cycle slips, $\bar{t}$, for a first-order Costas loop is given by the following equation for the unstressed loop case [*Hegarty*, 1997; *Holmes*, 1982]:

$$\bar{t} = \frac{\pi^2}{8\sigma^2_{\phi_\varepsilon} B_n} I_0^2\left(\frac{1}{4\sigma^2_{\phi_\varepsilon}}\right) \qquad (6)$$

where B_n is the loop bandwidth (10 Hz), and I_0 (•) is the modified Bessel function (order zero) of the first kind. Figure 10 shows the relationship between $\bar{t}$ and $\sigma_{\phi_\varepsilon}$ for a first-order loop. Higher-order loops, used for dynamic platforms, typically exhibit much smaller (two to three orders of magnitude) values of $\bar{t}$ versus $\sigma_{\phi_\varepsilon}$ [*Stephens and Thomas*, 1995].

[20] The second column of Table 1 contains the results of evaluating equation (6) for jitter values of 9 through 12 deg. These values are representative of a first-order PLL. The third column is two orders of magnitude smaller and represents the equivalent values for a third-order PLL based on simulation results from *Stephens and Thomas* [1995].

[21] From Table 1, it seems reasonable to select a threshold value of 10 deg since that will represent a

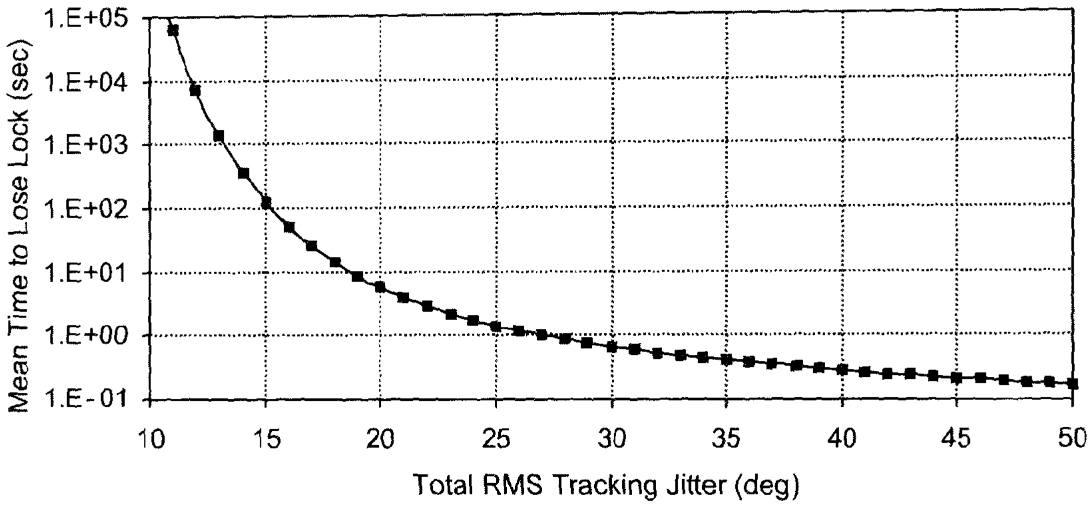

Figure 10. Mean time to lose lock versus total RMS tracking jitter.

mean time to lose lock of about 3 hours. Consequently, a long flight through CONUS might expect no more than one loss of lock over the duration of the flight in areas where loss of lock was not predicted. Therefore, if $\sigma_{\phi_\epsilon}(rad) \cdot \frac{180}{\pi} > t_p = 10$ degrees, the receiver is considered to have lost lock on L1-C/A due to carrier phase error.

3.4. Determining PLL Variance for Semicodeless L2 Receiver Aided by L1

[22] An exact determination of phase variance error for this case cannot be determined; however, minimum and maximum bounds can be determined based on whether there is respectively full correlation or no correlation between L1 and L2. This relationship is derived by *Conker et al.* [2000]. The process is shown in Figure 11 where λ_1, λ_2, = L1, L2 wavelenghts (m) and ϕ_1, ϕ_2 = L1, L2 carrier phases (radians).

[23] As before, the phase tracking error variance is the sum of the phase scintillation variance with respect to L2 plus the thermal noise and receiver oscillator noise or:

$$\sigma^2_{\phi_{\epsilon 2}} = \sigma^2_{\phi_{s,P2}} + \sigma^2_{\phi_T} + \sigma^2_{\phi,osc} \qquad (7)$$

However, for this case the thermal noise component is dependent on L1 and L2 as derived by *Conker et al.* [2000]:

$$\sigma^2_{\phi_T} = \frac{B_n\left[1+\frac{1}{2\eta_Y (c/n_0)_{L1P}\left(1-S_4^2(L1)\right)}\right]}{(c/n_0)_{L2P}\left(1-S_4^2(L2)\right)} \qquad (8)$$

where

B_n second-order PLL bandwidth, equal to 0.25 Hz;

$(c/n_0)_{L1P} = 10^{0.1(C/N_0)_{L1P}}$;

$(c/n_0)_{L2P} = 10^{0.1(C/N_0)_{L2P}}$;

η_Y GPS predetection time for Y code on L2, equal to 1.96×10^{-6} s;

$S_4(L1) < 0.687$.

Again in the case of no scintillation, $S_4(L1) = S_4(L2) - 0$ and (8) reduces to the standard representation for thermal noise [*Hegarty et al.*, 1999]:

$$\sigma^2_{\phi_T} = \frac{B_n}{(c/n_0)_{L2P}}\left[1 - \frac{1}{2\eta_Y (c/n_0)_{L1P}}\right]$$

The phase scintillation variance for L2 is:

$$\sigma^2_{\phi_{s,P2}} \cong 2\int_0^\infty |1-H(f)|^2 S_{\phi_2}(f)\,df \qquad (9)$$

Table 1. Mean Time to Lose Lock for Selected RMS Tracking Jitter Values

σ_ϕ, deg	$\bar{\tau}$ (First-Order PLL), hours	$\bar{\tau}$ (Third-Order PLL), hours
9	14,149.57	141.50
10	303.02	3.03
11	17.68	0.18
12	2.04	0.02

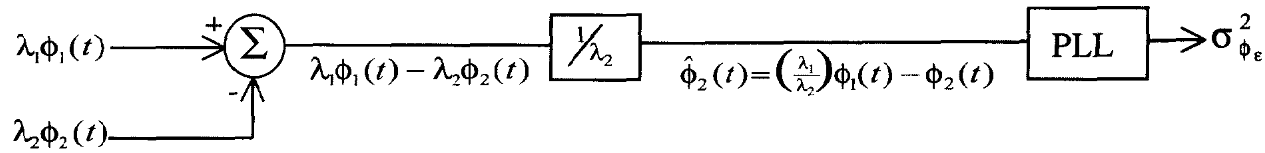

Figure 11. Semicodeless PLL.

A representation for $S_{\hat{\phi}_2}(f)$, the PSD of $S_{\hat{\phi}_2}(f)$, with respect to $S_{\phi_1}(f)$, the PSD of $\hat{\phi}_1$, is needed and is derived by *Conker et al.* [2000]. It is as follows:

$$S_{\hat{\phi}_2}(f) = \begin{cases} S_{\phi_1}(f)(\alpha^2 + 1/\alpha^2), \phi_1, \phi_2 \text{ uncorrelated} \\ S_{\phi_1}(f)(\alpha^2 + 1/\alpha^2 - 2), \phi_1, \phi_2 \text{ fully correlated} \end{cases} \tag{10}$$

where

$$\alpha = \frac{\lambda_1}{\lambda_2} = \frac{f_2}{f_1} = \frac{60}{77}.$$

Combining (7)–(10) and the approximation $S_{\phi_1}(f) \cong Tf^{-p}$, we have:

$$\sigma^2_{\hat{\phi}_2} = \frac{B_n\left[1 + \frac{1}{2\eta_Y (c/n_0)_{L1P}\left(1 - S_4^2(L1)\right)}\right]}{(c/n_0)_{L2P}\left(1 - S_4^2(L2)\right)} + \sigma^2_{\phi,OSC} + \frac{\pi T}{k f_n^{p-1} \sin\left(\frac{[2k+1-p]\pi}{2k}\right)} \cdot \begin{cases} (\alpha^2 + 1/\alpha^2), \textit{case A} \\ (\alpha^2 + 1/\alpha^2 - 2), \textit{case B} \end{cases} \tag{11}$$

where: case A = ϕ_1 and ϕ_2 are uncorrelated, case B = ϕ_1 and ϕ_2 are fully correlated, and $k = 2$ and $f_n = .075$ Hz [*Van Dierendonck*, 1996]. As before, if $\sigma_{\hat{\phi}_2}$ (rad) $\cdot$ (180/π) > $t_P = 10$ deg, the receiver is considered to have lost lock due to phase variance error.

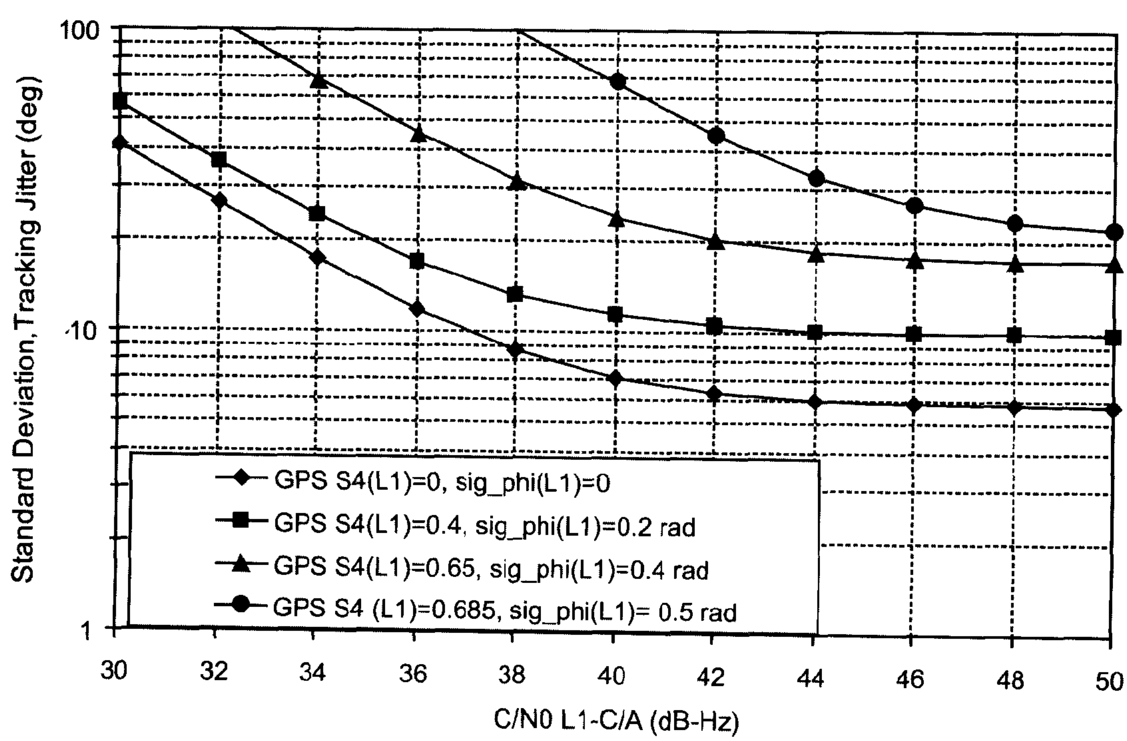

Figure 12. Standard deviation of the tracking jitter for L2 semicodeless aided by *L1 carrier* (GPS).

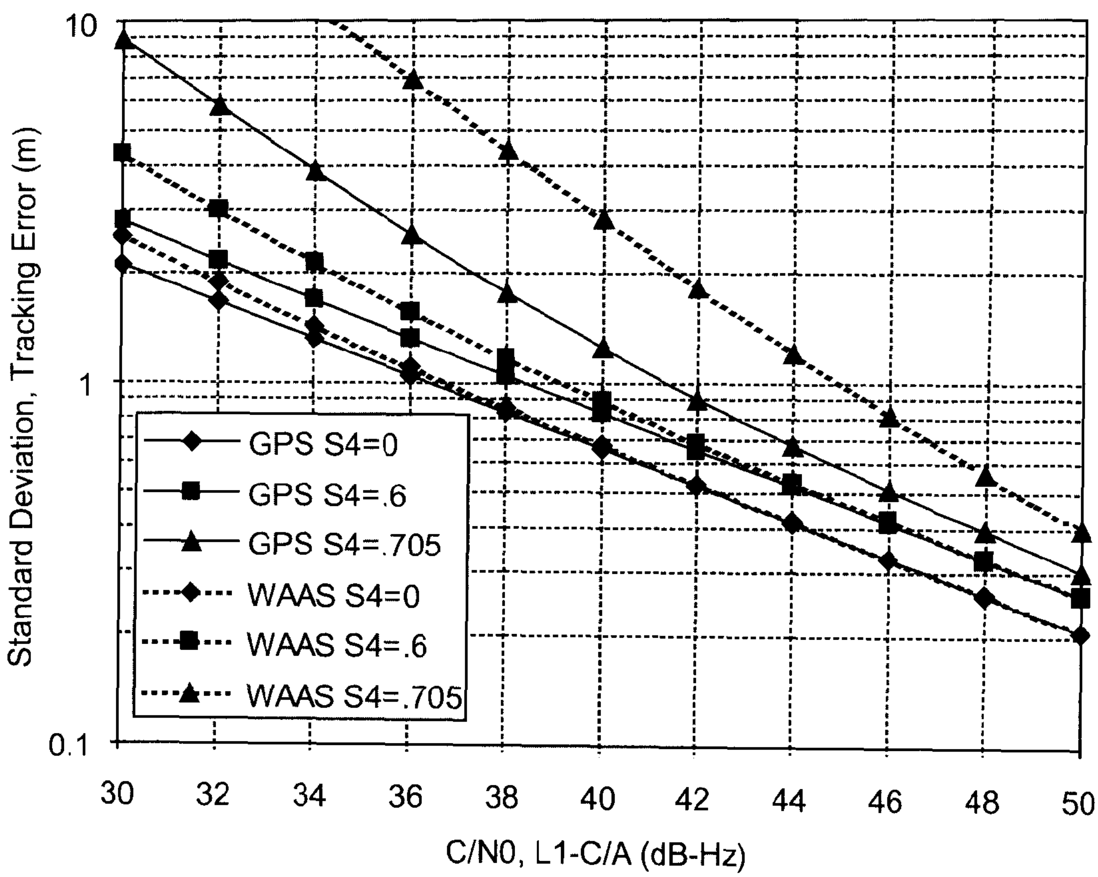

Figure 13. L1-C/A code tracking error (d = 1).

[24] Figure 12 shows the standard deviation of the tracking jitter for L2 semicodeless aided by L1 carrier using equation (11) for GPS.

3.5. Determining DLL Variance For L1 GPS and SBAS C/A Code

[25] Civilian GPS users are typically not interested in tracking code phase once carrier tracking is lost, since navigation data parity checking is used as a robust lock detector. However, if carrier tracking is not lost from amplitude or phase scintillation, the question becomes to what degree are code tracking errors (and therefore pseudorange errors) increased. Phase scintillations are ignored since they have little effect on code tracking errors. We need only concern ourselves with code tracking errors caused by thermal noise, interference, and amplitude scintillations.

[26] In the absence of scintillation, the tracking variance for a DLL, in C/A code chips squared, may be expressed as [*Hegarty et al.*, 1999]:

$$\sigma_\tau^2 = \frac{B_n d}{2(c/n_0)_{L1-C/A}}\left[1 + \frac{1}{\eta(c/n_0)_{L1-C/A}}\right] \qquad (12)$$

where B_n is the one-sided noise bandwidth, equal to 0.1 Hz (typical), and d is the correlator spacing in C/A chips, equal to 1 to 0.1 (typical).

[27] In the presence of scintillation, the thermal noise jitter variance, in C/A code chips squared, is:

$$\sigma_\tau^2 = \frac{B_n d\left[1 + \frac{1}{\eta(c/n_0)_{L1-C/A}\left(1-2S_4^2(L1)\right)}\right]}{2(c/n_0)_{L1-C/A}\left(1 - S_4^2(L1)\right)} \qquad (13)$$

This is derived in a manner completely analogous to the derivation of the thermal noise jitter variance for a PLL by *Conker et al.* [2000], by representing the jitter variance in terms of the scintillation amplitude and distributing the variance over the Nakagami-m distribution. Note that for the case of no scintillation, $S_4(L1) = 0$, and equation (13) becomes equation (12).

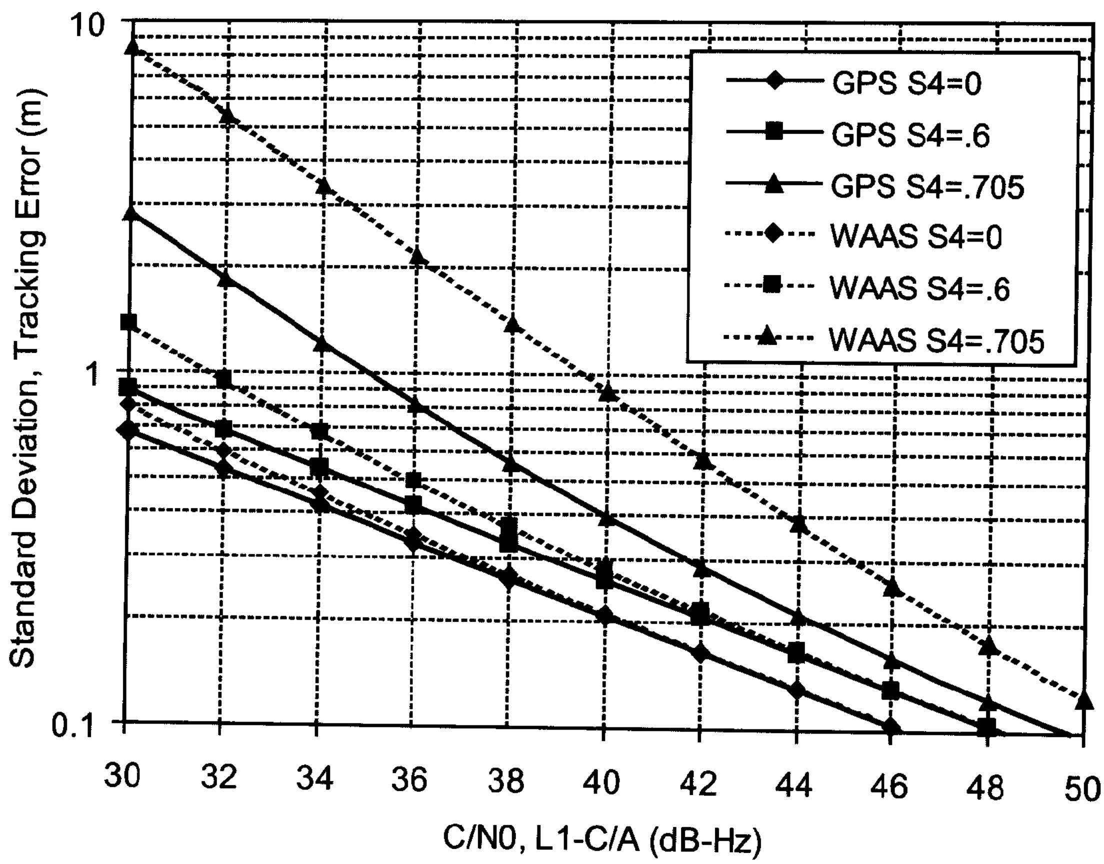

Figure 14. L1-C/A code tracking error (d = 0.1).

[28] The standard deviation of the DLL tracking jitter in meters is:

$$\sigma_{\hat{\tau}} = W_{CA}\sigma_{\tau},$$

where W_{CA} is the chip length for L1-C/A, equal to 293.0523 m.

[29] Figures 13 and 14 show respectively the results of L1-C/A code tracking for $d = 1$ and 0.1 for GPS receivers. Displayed are the values of $\sigma_{\hat{\tau}}$ with respect to $(C/N_0)_{L1\text{-}C/A}$ for different levels of ionospheric scintillation. The curve for $S_4(L1) = 0.705$ begins to diverge upward. This value was chosen since it is just below 0.707, and from equation (13) is not valid for $S_4(L1) \geq 0.707$. Of course, this does not present a problem, since according to our model, loss of lock occurs above this level in which case range errors are irrelevant.

3.6. Determining DLL Variance for L2 Semicodeless

[30] With no scintillation, the DLL jitter variance due to noise or wideband interference, in chips squared, for a semicodeless receiver is [*Hegarty et al.*, 1999]

$$\sigma_{\tau}^2 = \frac{B_n}{2(c/n_0)_{L2P}}\left[1 + \frac{1}{2\eta_Y(c/n_0)_{L1P}}\right] \tag{14}$$

where B_n is the one-sided bandwith, equal to 0.3 Hz. Once again in a manner analogous to that of *Conker et al.* [2000], we express the variance in terms of the scintillation amplitude for L1P and L2P and distribute this over the 2-D Nakagami-m distribution, which produces (in chips squared):

$$\sigma_{\tau}^2 = \frac{B_n\left[1 + \frac{1}{2\eta_Y(c/n_0)_{L1P}\left(1 - S_4^2(L1)\right)}\right]}{2(c/n_0)_{L2P}\left(1 - S_4^2(L2)\right)} \tag{15}$$

If scintillation is not present, $S_4(L1) = S_4(L2) = 0$, and equation (15) becomes equation (14). The standard deviation of the DLL tracking jitter in meters is:

$$\sigma_{\hat{\tau}} = W_P\sigma_{\tau}$$

where W_p is the chip length for P code, equal to 29.30523 m. The semicodeless code tracking results are

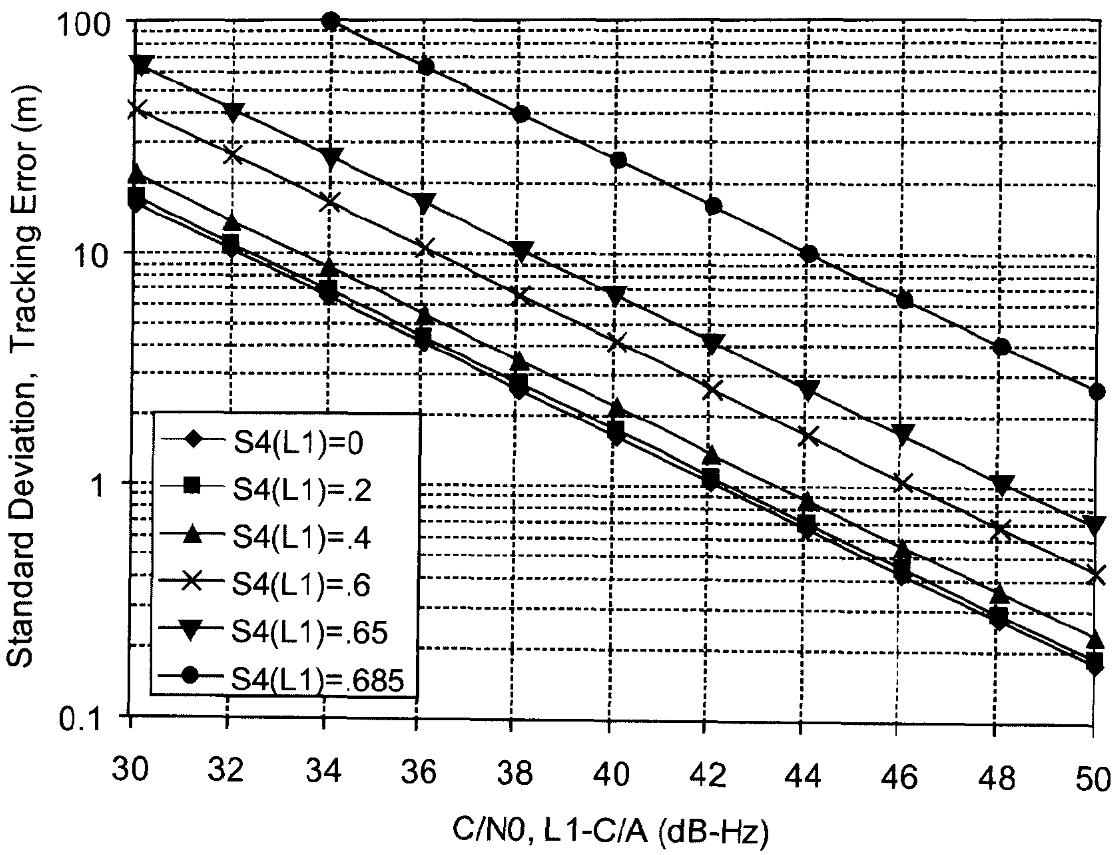

Figure 15. L2 semicodeless code tracking error.

shown in Figure 15, which depicts the standard deviation of the DLL tracking jitter against C/N_0 of L1-C/A in order to form a comparison with Figures 13 and 14. The ionospheric scintillation is expressed in terms of $S_4(L1)$. To construct this chart, the following relationships were used:

$$(C/N_0)_{L1P} \cong (C/N_0)_{L1-C/A} - 3dB$$
$$(C/N_0)_{L2P} \cong (C/N_0)_{L1-C/A} - 6dB$$
$$S_4(L2) = 1.454 S_4(L1).$$

The curve for $S_4(L1) = 0.685$ is shown deviating from the other curves since 0.685 is just below the point at which the equation is not defined. From *Conker et al.* [2000], this calculation is shown to be valid only for $S_4(L1) < 0.687$. Recall, however, that this is a threshold above which the model will determine that there is a loss of lock making range errors irrelevant.

4. Analysis of Peak Solar Cycle Scintillation in the Western Hemisphere

[31] Figure 16–19 represent the results of applying the above equations for phase angle error to L1 and L2 in the western hemisphere. The UTC time is 0400, which translates to a local time of 11:00 PM EST and 8:00 PM PST. These after sunset times represent a period when scintillation is at its maximum. The day chosen is February 21 with SSN = 150 and Kp = 1 representing the peak of the solar cycle but without the complication of an ionospheric storm.

[32] The first two charts depict the effects of scintillation on L1. Loss of lock is considered to have occurred at any time the phase angle threshold of 10 deg or the $S_4(L1)$ index of 0.707 is exceeded. The first chart, Figure 16, gives at each 5-deg grid increment the number of satellites that broadcast L1 and could be seen at that time and place. These totals include the two GEOs stationed at 54W and 178E. In Figure 17, the maximum number of satellites not locked is given. Subtracting the number of satellites in Figure 17 from the number of satellites of Figure 16 for the same position, the minimum number of satellites still in lock is obtained. The minimum availability of en route through nonprecision approach (NPA) service is obtained by assuming all satellites with large scintillation (ones whose phase errors exceed the 10-deg threshold or which exceed *the* $S_4(L1)$ *of 0.707)* will result in loss of lock. In practice, the probability of

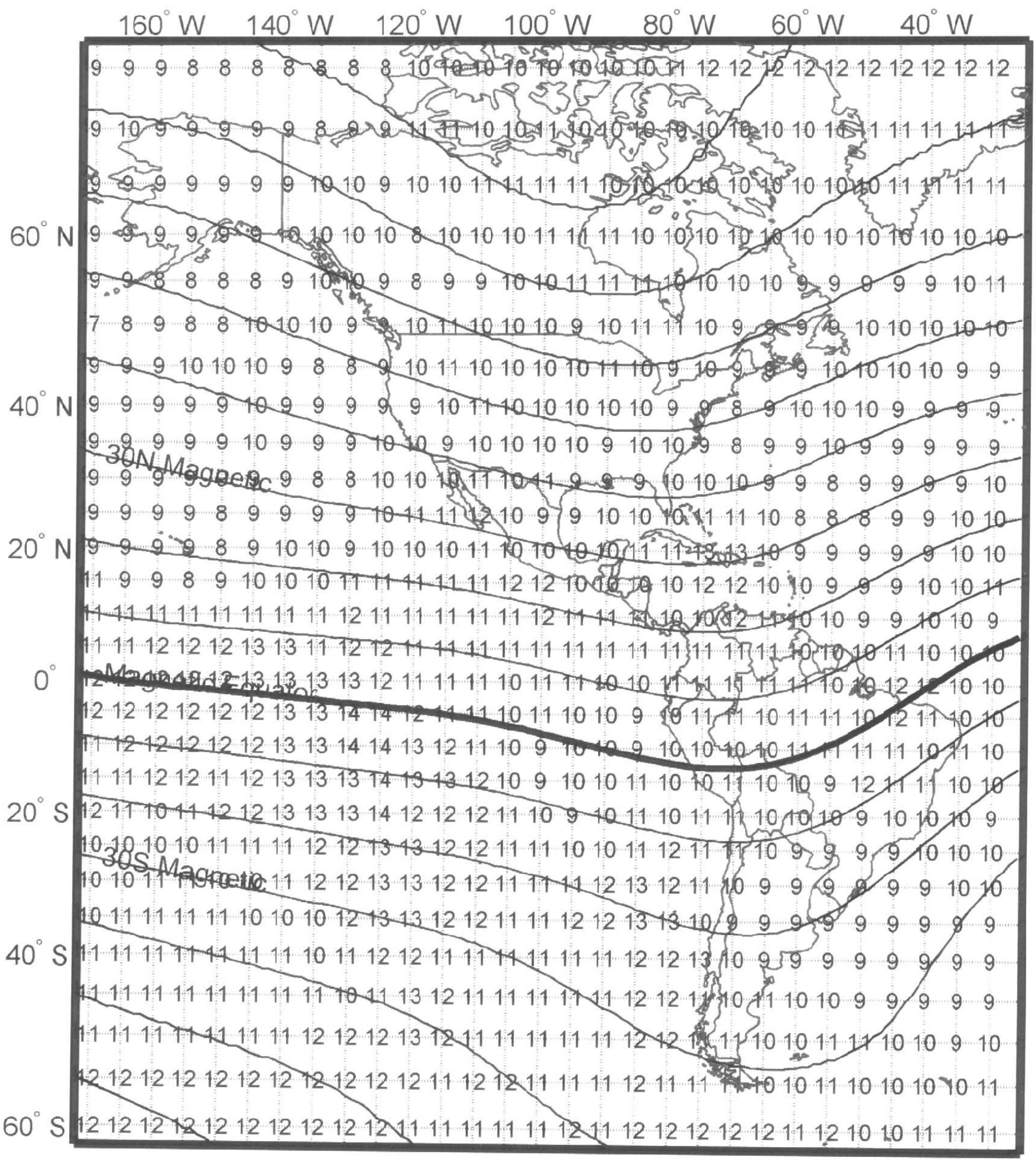

Figure 16. Number of satellites visible broadcasting L1-CA (27 GPS satellites; 2 Inmarsat GEOs; 5-deg mask angle; UTC = 0400).

losing lock on all satellites in any one location with large scintillation is very small.

[33] The second group of charts (Figures 18–19) are the same as the first two except that the totals apply to L2. The L2 signal received by the SBAS reference receiver is used to correct the pseudoranges caused by the delay through the ionosphere for precision approach applications. Both L1 and L2 must be tracked by a reference receiver for its measurement to be used by the SBAS master station. Loss of lock is considered to have occurred at any time the phase angle threshold of 10 deg or the $S_4(L1)$ index of 0.687 is exceeded. SBAS receiver lock is calculated for the fully correlated case and not for the uncorrelated case. The number of